Efficient control of ultrafast optical nonlinearity of reduced graphene oxide by infrared reduction

S. Bhattachraya, R. Maiti, A. C. Das, S. Saha, S. Mondal, S. K. Ray, S. N. B. Bhaktha, and P. K. Datta

Citation: Journal of Applied Physics **120**, 013101 (2016);
View online: https://doi.org/10.1063/1.4955140
View Table of Contents: http://aip.scitation.org/toc/jap/120/1
Published by the American Institute of Physics

Efficient control of ultrafast optical nonlinearity of reduced graphene oxide by infrared reduction

S. Bhattachraya, R. Maiti, A. C. Das, S. Saha, S. Mondal,[a] S. K. Ray, S. N. B. Bhaktha, and P. K. Datta[b]
Department of Physics, Indian Institute of Technology Kharagpur, Kharagpur 721302, India

(Received 13 April 2016; accepted 21 June 2016; published online 1 July 2016)

Simultaneous occurrence of saturable absorption nonlinearity and two-photon absorption nonlinearity in the same medium is well sought for the devices like optical limiter and laser mode-locker. Pristine graphene sheet consisting entirely of sp^2-hybridized carbon atoms has already been identified having large optical nonlinearity. However, graphene oxide (GO), a precursor of graphene having both sp^2 and sp^3-hybridized carbon atom, is increasingly attracting cross-discipline researchers for its controllable properties by reduction of oxygen containing groups. In this work, GO has been prepared by modified Hummers method, and it has been further reduced by infrared (IR) radiation. Characterization of reduced graphene oxide (RGO) by means of Raman spectroscopy, X-ray photoelectron spectroscopy, and UV-Visible absorption measurements confirms an efficient reduction with infrared radiation. Here, we report precise control of non-linear optical properties of RGO in femtosecond regime with increased degrees of IR reduction measured by open aperture z-scan technique. Depending on the intensity, both saturable absorption and two-photon absorption effects are found to contribute to the non-linearity of all the samples. Saturation dominates at low intensity ($\sim$127 GW/cm^2) while two-photon absorption becomes prominent at higher intensities (from 217 GW/cm^2 to 302 GW/cm^2). The values of two-photon absorption co-efficient ($\sim$0.0022–0.0037 cm/GW for GO, and $\sim$0.0128–0.0143 cm/GW for RGO) and the saturation intensity ($\sim$57 GW/cm^2 for GO, and $\sim$194 GW/cm^2 for RGO) increase with increasing reduction, indicating GO and RGO as novel tunable photonic devices. We have also explained the reason of tunable nonlinear optical properties by using amorphous carbon model. *Published by AIP Publishing*. [http://dx.doi.org/10.1063/1.4955140]

INTRODUCTION

Graphene is an atomically thin two-dimensional (2D) carbon allotrope which consists of sp^2-hybridized carbon atoms. It has been widely used in the development of electronic[1] and photonic[2] devices as well as in laser mode-locker[3] due to its extraordinary electron mobility,[4] tunable Fermi level,[5] broadband universal absorption,[6] ultrafast carrier dynamics,[7,8] and unique nonlinear optical (NLO) properties.[9,10] Graphene has also been proved to be a substantial candidate for higher harmonic generation,[11] optical frequency mixer[12] due to its large nonlinear susceptibility. But the challenges faced in many applications of graphene based materials are the solubility, the absence of bandgap, and the difficulty to fabricate it in large scales.

Graphene Oxide (GO) is a strongly hydrophilic intermediate product to form graphene chemically. It has attracted attention among the researchers due to its tunable electrical[13] and optical properties.[14,15] Moreover, its low-cost processing, large-scale production, solvent and substrate compatibility,[16,17] and the ease of functionalization in order to obtain certain novel properties makes it a useful candidate for various applications like energy storage devices,[18] transparent conducting electrodes,[19] photodetectors,[20] and light-emitting devices.[14] GO can be considered as pristine graphene decorated with oxygen functional groups. There are mainly four oxygen functional groups present in it,[21] with the epoxy and hydroxyl groups situated at the basal plane and the carbonyl and carboxyl decorate the edges.[22] The most striking feature of GO is that the electronic band structure can be tuned continuously by selectively modifying these functional groups. The amount and the type of oxygen functional groups can be controlled by reduction procedure. Hence, the physical properties of GO and reduced graphene oxide (RGO) depend on both, the synthesis and the reduction procedure. GO can be transformed from insulator to semiconductor and even further to a semimetal, as the band gap of GO can vary from 0.5 to 2.2 eV.[23] Furthermore, the change in nonlinear optical (NLO) properties of any material is directly related to its electronic band gap. Thus, it is possible to tune the optical nonlinearity of GO by tailoring the band gap through reduction.

There are several processes for synthesis and reduction of GO. Thermal annealing and chemical reduction are most commonly used reduction technique.[24] While thermal annealing is reported to produce small and wrinkled graphene sheets, the chemicals which are used as reducing agents are mostly toxic. To exfoliate large RGO sheets, we

[a]Currently address: Institute of Photonics and Electronics of the CAS, Czech Republic.
[b]Author to whom correspondence should be addressed. Electronic mail: pkdatta.iitkgp@gmail.com. Current address: Dipartimento di Mathematica e Fisica, UniversitaCattolica del SacroCuore, Via Musei 41, I-25121 Brescia, Italy.

deploy the infrared (IR) irradiation on the solution phase of GO. IR radiation as a reduction technique also has the merits of being green, easy to scale, and cost effective. Previously, broadband NLO properties of GO dispersed in organic and inorganic solvents have been reported in nanosecond and picosecond regimes.[25] The GO films and chemically reduced RGO films have shown high optical limiting properties in the femtosecond regime.[26] Evidence of saturable absorption (SA) in solution processed few layered GO has also been reported.[27] A study has shown that metal oxide nanoparticle incorporated in GO/RGO sheets has increased charge transfer,[28] which may result in increasing optical nonlinearity. Chemical reduction has been used to tune the optical nonlinear property of GO in picosecond regime.[29] The cause of NLO properties in GO and RGO has been described predominantly in terms of saturable absorption (SA) and two photon absorption (TPA) due to their large values in the near IR range. But the cause of NLO property in RGO has not been clearly addressed so far, and the effect of different reduction procedures is still a matter of debate. Thus, to have a precise control over ultrafast NLO property of GO in colloidal solution in femtosecond regime, we have used IR irradiation as a controlling parameter which has not been studied so far.

Novel infrared (IR) induced reduction technique is used to prepare the samples, because it is a relatively slow process allowing us to measure easily the optical nonlinearity at each step. Chemically synthesized GO sample has been used to prepare various RGO samples with increasing degree of reduction. The nonlinear absorption properties of these samples measured by femtosecond z scan show SA at low intensity ($\sim$127 GW/cm^2), whereas TPA dominates at higher intensities (>200 GW/cm^2). The TPA coefficient and saturation intensity are also found to increase with the increasing reduction. An amorphous carbon model is used to explain the reason of tunable NLO properties by reduction.

SAMPLE PREPARATION

RGO samples are fabricated by impinging infra-red radiation using a broadband IR bulb (800–2200 nm) on GO. The modified Hummer method[30] is used to prepare an aqueous solution of GO of concentration 0.8 mg/ml by following the steps of oxidation, sonication, and centrifugation. Briefly, in this process, $KMnO_4$ is used as an oxidizing agent in the presence of H_2SO_4, which acts as an intercalating agent for the layered GO. Centrifugation is carried out to separate out the un-exfoliated graphite particle. The thickness of GO sheets is confirmed by performing AFM analysis on them. The as-grown GO solution is reduced by exposing it to a broadband (800–2000 nm) IR source for different periods of time in ambient condition.[31] The intensity of the radiation is controlled by adjusting the distance between the sample and the IR source. The GO solutions are kept at a distance of 5 cm (0.64 W/cm^2) from the source, for 60 min, 120 min, and 180 min to get three RGO samples (RGO1, RGO2, and RGO3) with increasing degree of reduction. The main underlying mechanism for the reduction of GO due to IR irradiation is photo-thermal effect.[32] The carbon based materials absorb IR irradiation, which results in phonons which in turn enhance the capability of these materials to efficiently convert light into thermal energy. Photothermal therapy can be given as an example where graphene oxide has been used to heat and kill cancer cells with low dosages of IR radiation.[33] The released heat during the reduction of GO has been found roughly ten times that necessary for the deoxygenation reaction, which causes a self-propagating domino-like deoxygenation reaction of the partially heated GO.[34] The temperature has been observed to increase with increasing exposure time when IR irradiation is done on GO coated thermocouple.[32] When the aqueous solution of GO is exposed to IR light, a gradual change in color from brownish-yellow to black can also be observed with the increased exposure time. The photographs of the dispersed samples are shown in Figure 1, and they have been observed to remain in the uniform colloidal state for 60 days.

EXPERIMENTAL METHODS

The samples are characterized by Raman spectroscopy, X-ray photoelectron spectroscopy (XPS) (PHI 5000 VersaProbe II, ULVAC-PHI, Inc., Japan), and UV-Visible absorption spectroscopy (Perkin ElmarLamda-900) to verify the degree of reduction of GO. For, XPS and Raman measurements, samples were drop casted on a pre-heated quartz substrate and dried subsequently. The micro-Raman measurements are carried out with argon-krypton mixed ion gas laser ($\lambda = 514$ nm) in back scattering geometry using a spectrometer, equipped with a microscope (model BX41 Olympus, Japan), triple monochromator (model T64000, JY, France), and a Peltier cooled CCD detector. The XPS measurement is done using A1-K_α x-ray of energy 1486.6 eV. Quartz cuvette of path length 1 mm is used for each RGO dispersion to measure the absorption spectrum by UV-VIS spectrophotometer. AFM image and section analysis shown in Figure 2 confirm the thickness of few layered GO flakes to be in the range of 8–12 nm.

The nonlinear optical measurements are carried out by a single beam z-scan technique.[35] The open aperture (OA) z-scan measurements are performed with a laser pulse of 150 fs at 1 kHz repetition rate at the wavelength of 808 nm (Coherent Libra-He). The as-grown GO and three other RGO samples in aqueous dispersion with increasing degree of reduction are used for the characterizations. The fs laser beam is focused to 58 μm (beam diameter) with a 20 cm

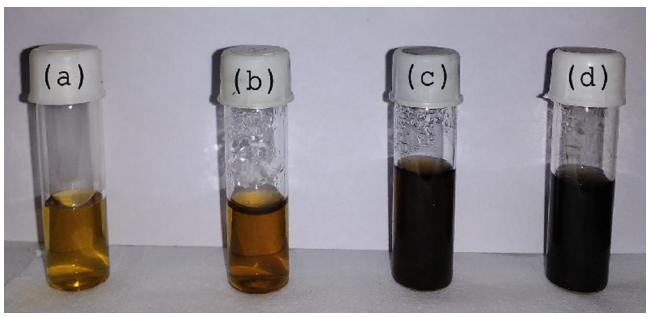

FIG. 1. Photographs of graphene oxide (GO) and reduced graphene oxide (RGO) dispersion used for nonlinear optical studies where (a), (b), (c), and (d) stand for as grown GO, RGO1 (reduced for 60 min), RGO2 (reduced for 120 min), and RGO3 (reduced for 180 min) dispersion, respectively.

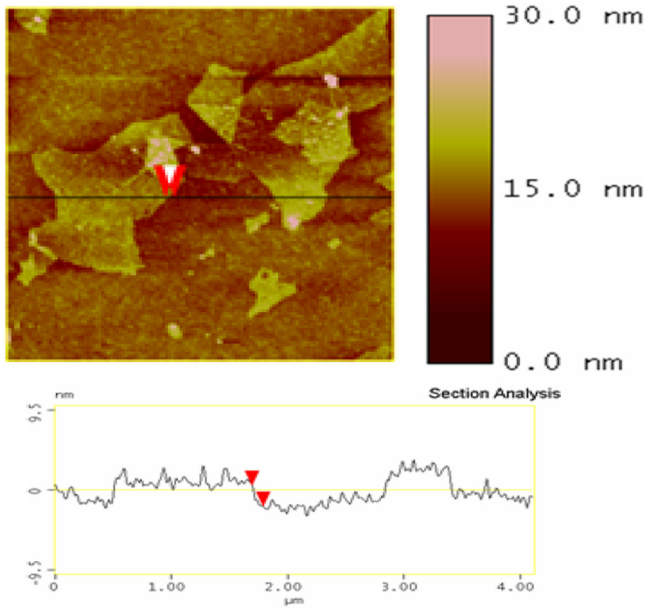

FIG. 2. AFM image of as-grown graphene oxide (GO) flake and the corresponding height profile.

plano-convex lens. RGO dispersion placed in the cuvette of 1 mm path-length is moved across the focus using a motorized translation stage (Thorlab, LTS-150). The Rayleigh range (z_0) of the focused beam is 1.1 cm, which is longer than the path-length of the beam in the cuvette. The input pulse power is varied with a combination of half-wave plate and a polarizer. The reference and the transmitted laser pulses are detected using two Si-photodiodes (Thorlab, PDA10A), and the data are recorded through a lock-in amplifier for better signal-to-noise ratio. The lock-in amplifier is triggered by a 1 kHz signal and is synchronized with the femtosecond laser pulse. The lock-in amplifier and

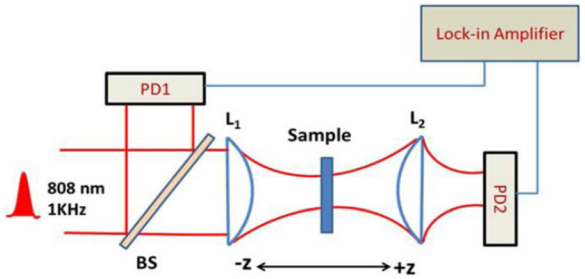

FIG. 3. Schematic of the z-scan experiment set-up. BS: Beam Splitter, L1 and L2: lens, PD1 and PD2: Si photodiode.

motorized translational stage are incorporated in LabVIEW environment for automation and averaging of data. Pulse-to-pulse fluctuation is taken care of using reference data from photodiode. Before taking measurements, the z-scan set up is calibrated using a slandered sample (CS_2). A schematic of the z scan experimental set-up is shown Figure 3.

RESULTS AND DISCUSSION

Spectroscopic studies (XPS, Raman, and linear absorption)

XPS is used to inspect the gradual de-oxygenation of GO with respect to the increasing exposure time of IR radiation. Though we have used XPS spectroscopy to characterize the oxygen functional groups, EPR spectroscopy has also been used to find out hybridization of carbon atoms in GO and also in other system such as carbon doped superconducting materials.[36] EPR study have also shown the effect of Mn ions in GO arising due to use of $KMnO_4$ in modified Hummer method.[37] XPS spectra from GO and RGO dispersions are shown in Figures 4(a)–4(d). The deconvoluted peaks from the C1s spectra of the as grown GO

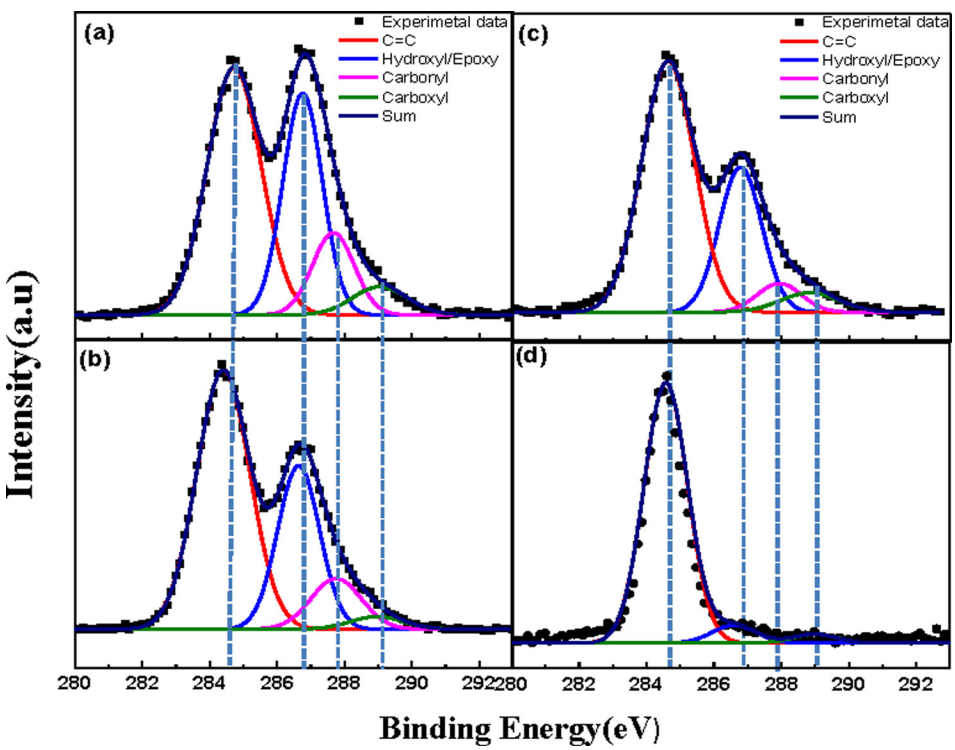

FIG. 4. High resolution XPS spectra of C1s for (a) as grown GO, (b) RGO1, (c) RGO2, and (d) RGO3.

TABLE I. Linear absorption coefficient and percentage area of sub-peaks of the fitted XPS spectra from all the samples.

Parameters	GO	RGO1	RGO2	RGO3
α linear absorption coefficient (cm^{-1}) at 808 nm	0.63	1.11	2.1	3.9
C=C	49.27%	57.76%	60.66%	90.54%
C-O/C-OH [epoxy/hydroxyl]	32.31%	28.78%	28.24%	6.29%
C=O [carbonyl] and C(=O)-OH [carboxyl]	18.39%	13.44%	11.03%	3.16%

are assigned to C=C/C-C bonds (284.6 eV), epoxy (C-O)/hydroxyl (C-OH) bonds (286.6 eV), carbonyl (C=O) bonds (287.9 eV), and carboxyl (C(=O)-OH) bonds (289.2 eV), which are also been reported previously.[38] The percentage area of each sub-peak has been calculated and tabulated in Table I. As seen from the XPS spectra, with the increment of exposure time, a gradual removal of oxygen containing groups in RGO is observed as expected. For the as-grown GO, C1s XPS spectrum consists of 49.27% of sp^2 hybridized carbon due to the C=C bonds, 32.1% of carbon atoms due to the C-O bonds, and 18.39% of carbon atoms due to (C=O) the carbonyl groups and carboxylic groups. The epoxy and hydroxyl groups are mainly situated in the basal plane whereas the carbonyl and carboxylic groups primarily decorate the edges of GO sheets. For a reduction time of 180 min (RGO3), atomic percentage of sp^2 hybridized carbon atom reaches 90% which in turn confirms efficient reduction. However gradual decrements of epoxy/hydroxyl group (6.29%) and carboxyl/carbonyl (3.16%) are also observed, which suggest that most of the oxygen functional groups are removed from the GO. To quantify the achievable reduction, in Figure 5, we have shown a plot on the evolution of C=C and epoxy/hydroxyl group as a function of reduction time.

The micro-Raman spectra of the as-deposited GO sheets and RGO sheets are shown in Figure 6. The Raman spectra of the samples shows two prominent characteristics peaks corresponding to the G-band (1602 cm^{-1}) and D-band (1352 cm^{-1}), respectively. The G-band is assigned to the

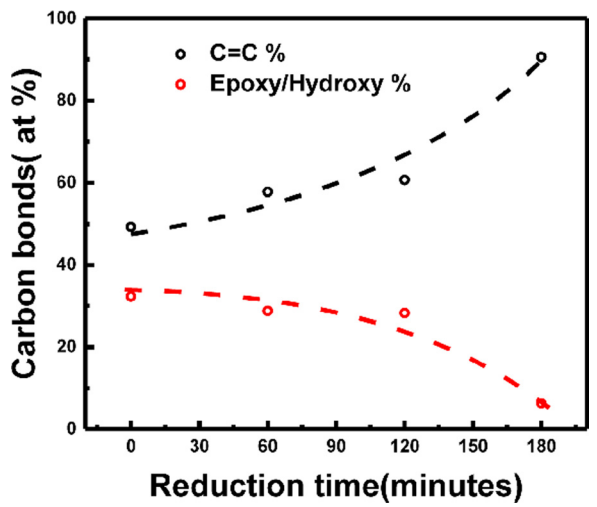

FIG. 5. The evolution of C=C and hydroxyl/epoxy groups as a function of reduction time. Dashed lines are guide to the eye.

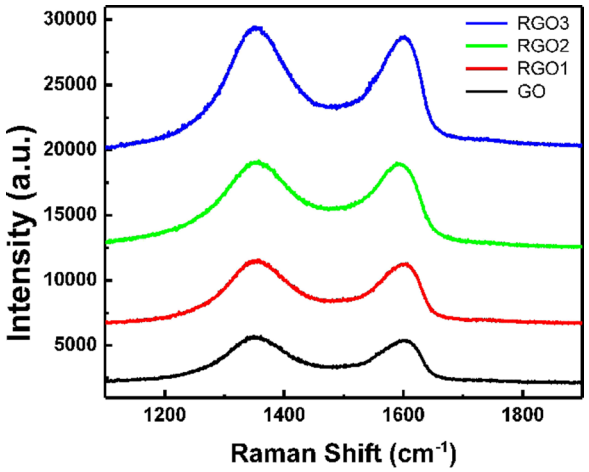

FIG. 6. Raman spectrum of as grown GO, RGO1, RGO2, and RGO3 with pump at 514 nm. The spectra are vertically shifted for clarity.

E2g phonon vibration of carbon sp^2 atoms, while the D-band is A1g breathing mode of carbon associated with structural defects and disorders.[39] The intensity ratios (I_D/I_G), which is the ratio of the integrated area for the two Raman bands of GO, RGO1, RGO2, and RGO3 dispersions, are calculated to be 1.74, 1.75, 1.85, and 1.9, respectively. Almost constant value of I_D/I_G suggest that the size of average sp^2 hybridized carbon cluster shows negligible variation from GO to partially reduced GO. It has been previously reported that the thermal reduction modifies the functional groups from GO, which causes the formation of new sp^2 domain within the sp^3 matrix. It also removes some carbon atoms in the form of the evolution of CO_2.[40] These two factors do not lead the sp^2 domain size of GO to change significantly after partial reduction.

The linear absorption properties of the as-grown GO and RGO, with different degrees of reduction by exposure of IR radiation, are studied by UV-Visible absorption measurements, and the resulting spectra are shown in Figure 7. All the samples exhibit an absorption peak in the UV (~235 nm). The absorption peak of GO at 230 nm is assigned to (C=C) transition whereas the shoulder at around 300 nm is due to n-π^* transition.[41] Plasmonic peak at 230 nm for GO is red-shifted with increasing reduction. Also, an overall increase in absorbance is observed with higher degree of reduction which is similar to the previously reported results.[42] The red shift of the absorption peak suggests the increment of atomic percentage in sp^2 hybridized carbon atom which is also consistent with the XPS results. Furthermore, the overall increase in absorbance also indicates the restoration of electronic conjugation with increasing reduction.[43]

CONTROL OF OPTICAL NONLINEARITY

The nonlinear optical properties of GO and RGO samples are studied using an open aperture (OA) z-scan technique. The results of the measurements are shown in Figure 8. The closed aperture z scan measurement of GO and RGO samples has also been done. But those curves are very close to pure di-ionized water and are not been reported here. For all the samples, the OA measurements are carried out at four different input pulse energies, 1.5 μJ, 2.5 μJ, 3.0 μJ, and 3.5 μJ.

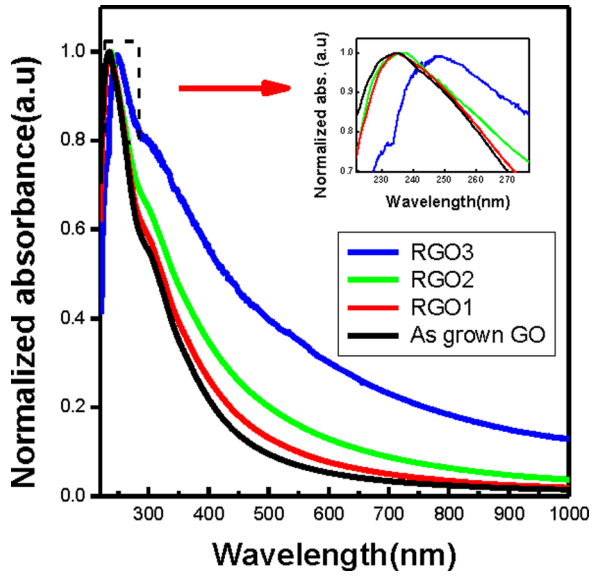

FIG. 7. UV-Visible absorption spectrum for as-grown GO, RGO1, RGO2, and RGO3. The inset shows the redshift of plasmonic peak with increasing reduction.

In the case of OA measurement, pure di-ionized water does not show any significant nonlinear absorption in the above mentioned input pulse energies. At lower pulse intensities, the OA curve shows saturation absorption (SA) behavior along with a dip appearing at the focus. The dip becomes more prominent, and the samples exhibit multi-photon absorption behavior with the increase in input pulse energies. Thus, we can predict that both SA and multi-photon absorption play crucial roles in the mechanism of nonlinear absorption.

To understand the z-scan results, we consider SA and two-photon absorption (TPA) simultaneously in the analysis.[25] A single Gaussian beam with a beam waist of w_0 can be represented as

$$I(z,r) = \frac{I_0}{1+\left(z^2/z_R^2\right)} \exp\left(-\frac{2r^2}{w^2(z)}\right) \exp\left(-\frac{t^2}{\tau_p^2}\right), \quad (1)$$

where I_0 is the on-axis intensity at focus, $z_R(\pi w_0^2/\lambda)$ is the Rayleigh length, τ_p is the pulse-width of input pulse, and $w(z)$ can be defined as $w^2(z) = {w_0}^2(1+z^2/z_R^2)$. The propagation of laser beam within the sample can be determined from the intensity equation

$$\frac{dI}{dz} = -\alpha(I)I, \quad (2)$$

where $\alpha(I)$ is the intensity dependent absorption coefficient. For an in-homogeneously broadened two-level system with both SA and TPA, $\alpha(I)$ can be written as

$$\alpha(I) = \frac{\alpha_0}{1+\frac{I}{I_{Sat}}} + \beta_{eff} I, \quad (3)$$

where I_{Sat} is the saturation intensity and β_{eff} is the TPA coefficient.[44] The transmittance of the incident laser beam is obtained by solving Equation (2) with $\alpha(I)$ from Equation (3), and by integrating it over time and radial direction. The intensity equation has been solved numerically using Crank-Nichelson method. Assuming the input beam to be Gaussian, the integration limits of t and z are varied from $-\infty$ to $+\infty$ and 0 to ∞, respectively. The theoretical fits of the obtained data resulted in

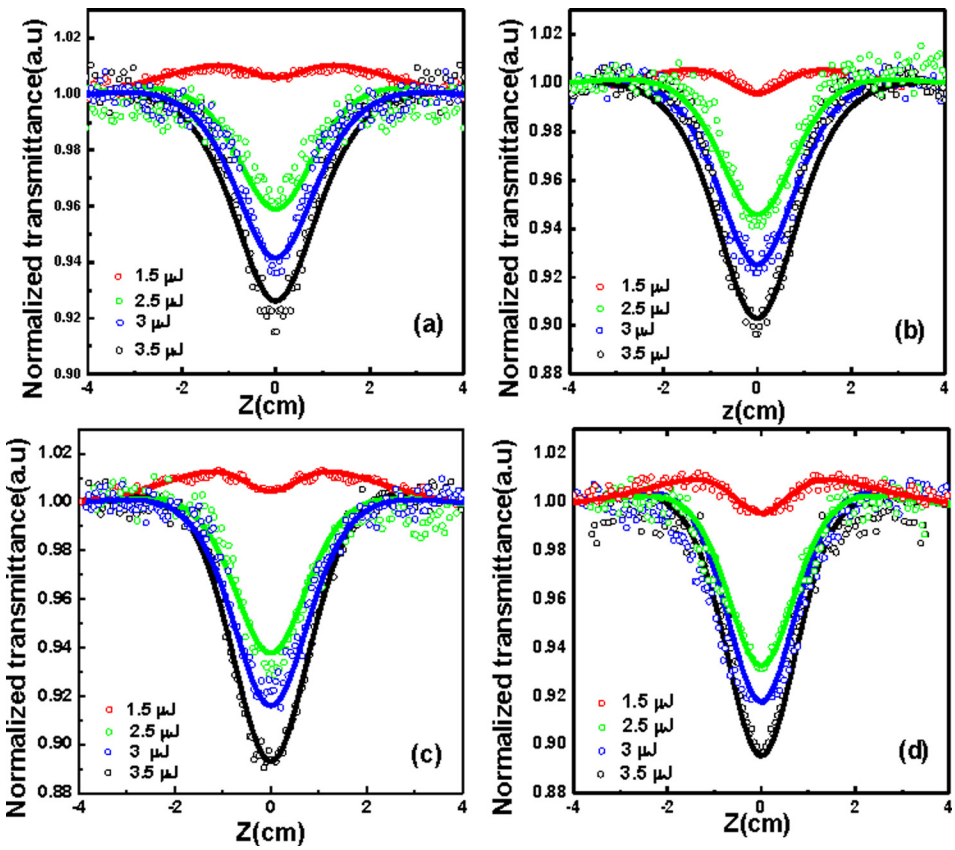

FIG. 8. Open aperture z-scan curves of (a) as-grown GO, (b) RGO1, (c) RGO2, and (d) RGO3 at different input pulse energies. The experimental data are represented by the open colored symbols and the solid curves denote the fitted plots.

TABLE II. Parameters derived from fitting of open-aperture Z-scan data.

Input pulse energy (μJ)	GO		RGO1		RGO2		RGO3	
	I_{sat} (GW/cm^2)	β_{eff} (cm/GW)	I_{sat} (GW/cm^2)	β_{eff} (cm/GW)	I_{sat} (GW/cm^2)	β_{eff} (cm/GW)	I_{sat} (GW/cm^2)	β_{eff} (cm/GW)
1.5	57	0.0022	94	0.0047	137	0.0072	194	0.0128
2.5	57	0.0037	94	0.0062	137	0.0093	194	0.0143
3	57	0.0043	94	0.0064	137	0.0094	194	0.0136
3.5	57	0.0044	94	0.0065	137	0.0095	194	0.0131

the determination of the values of I_{Sat} and β_{eff}. The values corresponding to the RGO dispersions under study are summarized in Table II. A dimensionless figure of merit (FOM) for nonlinear absorption has also been defined as FOM $= \beta_{eff} I_{Sat}/\alpha_o$. The values of FOM for GO and RGO dispersions at different input pulse energies has been tabulated in Table III.

From Table II, we observe that β_{eff} increases with the input pulse energies for a particular sample. Though we have modeled the nonlinear absorption using only SA and TPA, there may be a possibility of higher order multi-photon absorptions occurring in the samples. Variations of TPA coefficient (β_{eff}) with input peak intensity for all the samples have been plotted in Figure 9. Previously reported results concluded that the slight increase in β_{eff} with increasing pulse energies may be attributed to the excited state absorption at higher intensities.[45] But, for this process to occur, the lifetime of the excited state absorption has to be of the same order as the time between two consecutive laser pulses, in order to prevent complete relaxation from the excited state to the ground state. In our case, we used laser pulses of 150 fs at 1 kHz repetition rate. Thus, the time between two consecutive pulse (∼ms) is much larger that the lifetime of the excited state (∼ps)[46] ruling out the possibility of excited state absorption. However, at higher intensities, there may be a possibility of two-step multi-photon absorption. Furthermore, we observe that not only the linear transmission coefficient but also β_{eff} and I_{Sat} increase with the increasing degree of reduction of GO. Thus, nonlinear absorption property of RGO dispersions can be efficiently controlled with photo-thermal reduction.

GO has a unique atomic and electronic structure. Previously, the amorphous structural carbon model has been used to understand the nonlinear absorption property of GO and RGO.[47] During the preparation of GO, due to the oxidation of graphite, patterned aromatic rings of sp^2 hybridized carbon clusters are formed. According to the model, amorphous aggregation of oxygen containing groups form a sp^3 matrix in which sp^2 cluster islands are buried. These sp^2 carbon clusters are isolated by sp^3 matrix. When the reduction takes place with increasing exposure time of IR radiation, oxygen functional groups are gradually removed from the basal plane, thus creating small sp^2 hybridized domains. With the increment of reduction, larger and newer sp^2 domains are created, though the size of sp^2 clusters remains the same. As the electronic band-gap of sp^2 hybridized carbon atoms change with size (no. of aromatic rings), the band-gap of newly created sp^2 domains can typically vary from 0.5–6.0 eV.[23] However, in sp^3 matrix (where carbon atoms are connected with oxygen functional group), a larger band-gap is observed (∼2.7 eV or 6.0 eV).[48,49] In Figure 10, a cartoon diagram is used to show the effect of gradual photo-thermal reduction on GO and the evolution sp^2 domain. In our case, we used the pump photon of 1.51 eV (808 nm). So, when input pulse power is low, the electrons in the ground state of as-prepared GO and RGO samples experience Pauli blocking in sp^2 clusters or sp^2 domain or in both and saturate the band-gap resulting in SA. But TPA and multi-photon absorption may occur from sp^3 matrix as well as sp^2 domains. With increased reduction, the fractional number of sp^2 hybridized carbon atoms increases, which in turn explains the increment of I_{Sat} with reduction. Though β_{eff} depends on the number of carbon sites and TPA cross section, the total number of carbon sites remains a constant after the reduction of sp^3 matrix into sp^2 domains. Thus, the

TABLE III. Figure of Merit (FOM) of nonlinear absorption in GO and RGO dispersions at different input pulse energies. Values have been rounded as per accuracy of the measurement.

Input pulse energy (μJ)	GO FOM	RGO1 FOM	RGO2 FOM	RGO3 FOM
1.5	0.199	0.398	0.470	0.637
2.5	0.335	0.525	0.607	0.711
3	0.389	0.542	0.613	0.676
3.5	0.398	0.550	0.620	0.652

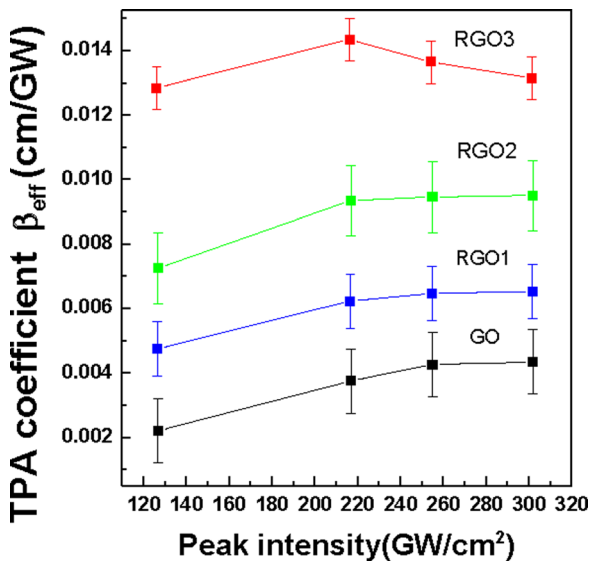

FIG. 9. Variation of TPA coefficient with input peak intensity for GO, RGO1, RGO2, and RGO3 dispersion.

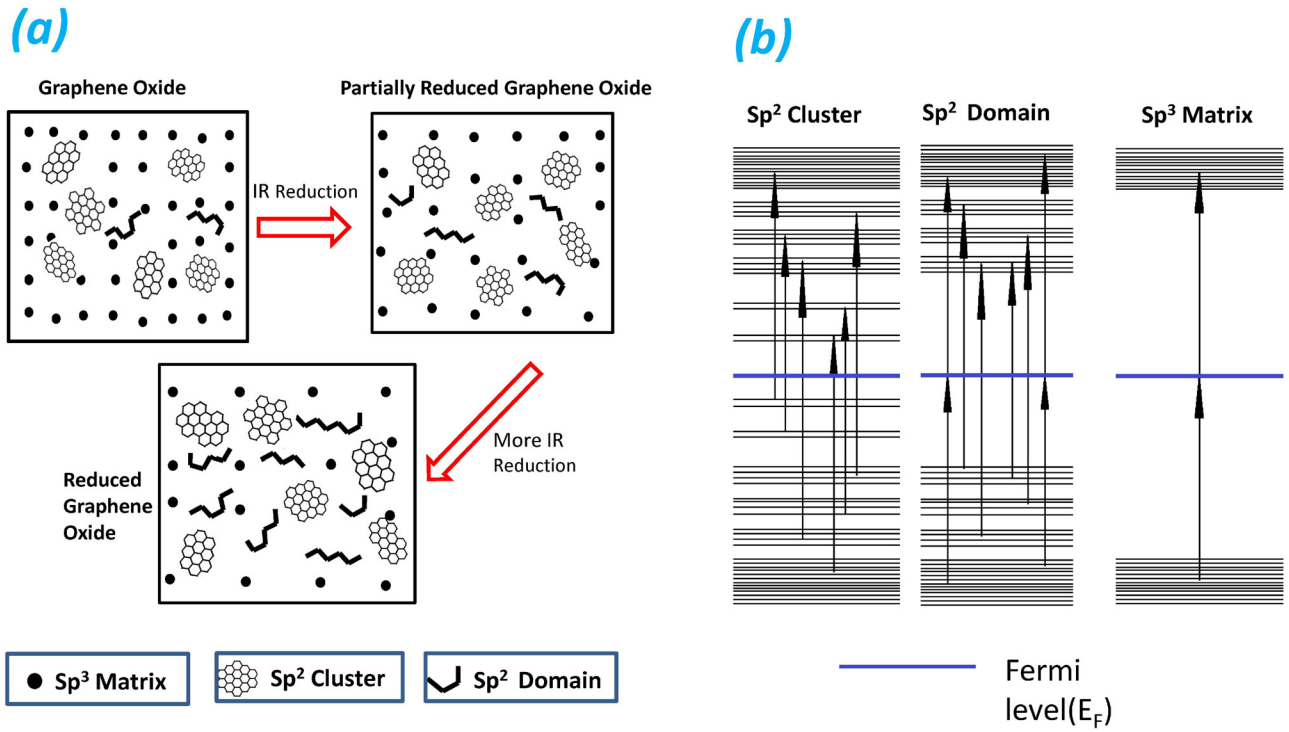

FIG. 10. A cartoon diagram on the (a) effect of IR radiation on GO and the evolution of sp^3 matrix and sp^2 domains, (b) possible transitions from sp^3 cluster, sp^2 domain, and sp^3 matrix.

increment in β_{eff} with reduction solely indicates that TPA cross-section of sp^2 domain is higher than sp^3 matrix.

CONCLUSIONS

GO is efficiently de-oxygenated to obtain RGO by irradiation of IR beam. Reduction is confirmed by high resolution XPS measurements. Optical nonlinearities of GO reduced at different degrees are measured by an open aperture Z-scan with a femtosecond laser pulse at 808 nm. The saturation intensity and two-photon absorption coefficients are determined and are found to increase with the degree of reduction. The results are accounted with amorphous carbon model and are further supported with other analytical results like linear absorption, XPS, and micro-Raman studies.

Based on the above results, it may be inferred that RGO can be used as a saturable absorber up to the intensity level of 100 GW/cm^2 in a wavelength range above 500 nm with dynamic response in picosecond time scale. The material may be ideal for passive Q-switching and mode-locking of laser as the saturation intensity and the depth of modulation can be tuned with the degree of reduction. Moreover, the availability of forward saturation and reverse saturation[50] due to TPA may make RGO an ideal candidate for mode-locking from the stability point of view as the reverse saturation mimics the negative feedback to the laser cavity. As the saturation intensities are not very high, this may be suited for diode-pumped low-power sub-picosecond systems useful for photochemistry.

ACKNOWLEDGMENTS

The authors acknowledge SGDRI scheme (UPM project) of IIT Kharagpur for the necessary equipment support for the work. DST-FIST project is acknowledged for the XPS measurements at the Department of Physics, IIT Kharagpur. P.K.D. acknowledges ICTP, Trieste for subsistence support. The authors like to acknowledge Dr. Francesco Banfi and Dr. Luca Gavioli, Universita Cattolica del Sacro Cuore, Brescia, Italy, for useful discussions.

[1]Q. Bao and K. P. Loh, "Graphene photonics, plasmonics, and broadband optoelectronic devices," ACS Nano **6**, 3677–3694 (2012).
[2]F. Bonaccorso, Z. Sun, T. Hasan, and A. C. Ferrari, "Graphene photonics and optoelectronics," Nat. Photonics **4**, 611–622 (2010).
[3]A. Martinez and Z. Sun, "Nanotube and graphene saturable absorbers for fibre lasers," Nat. Photonics **7**, 842–845 (2013).
[4]S. V. Morozov, K. S. Novoselov, M. I. Katsnelson, F. Schedin, D. C. Elias, J. A. Jaszczak, and A. K. Geim, "Giant intrinsic carrier mobilities in graphene and its bilayer," Phys. Rev. Lett. **100**, 016602 (2008).
[5]Y. Zhang, T. T. Tang, C. Girit, Z. Hao, M. C. Martin, A. Zettl, M. F. Crommie, Y. R. Shen, and F. Wang, "Direct observation of a widely tunable bandgap in bilayer graphene," Nature **459**, 820–823 (2009).
[6]K. F. Mak, M. Y. Sfeir, Y. Wu, C. H. Lui, J. A. Misewich, and T. F. Heinz, "Measurement of the optical conductivity of graphene," Phys. Rev. Lett. **101**, 196405 (2008).
[7]J. M. Dawlaty, S. Shivaraman, M. Chandrashekhar, F. Rana, and M. G. Spencer, "Measurement of ultrafast carrier dynamics in epitaxial graphene," Appl. Phys. Lett. **92**, 042116 (2008).
[8]M. Breusing, C. Ropers, and T. Elsaesser, "Ultrafast carrier dynamics in graphite," Phys. Rev. Lett. **102**, 086809 (2009).
[9]G. Lim, Z. Chen, J. Clark, R. G. S. Goh, W. Ng, H. Tan, R. H. Friend, P. K. H. Ho, and L. Chua, "Giant broadband nonlinear optical absorption response in dispersed graphene single sheets," Nat. Photonics **5**, 554–560 (2011).
[10]H. Zhang, S. Virally, Q. Bao, L. K. Ping, S. Massar, N. Godbout, and P. Kockaert, "Z-scan measurement of the nonlinear refractive index of graphene," Opt. Lett. **37**, 1856–1858 (2012).
[11]J. J. Dean and H. M. Van Driel, "Second harmonic generation from graphene and graphitic films," Appl. Phys. Lett. **95**, 261910 (2009).
[12]A. Y. Bykov, T. V. Murzina, M. G. Rybin, and E. D. Obraztsova, "Second harmonic generation in multilayer graphene induced by direct electric current," Phys. Rev. B **85**, 121413 (2012).

[13]I. Jung, D. A. Dikin, R. D. Piner, and R. S. Ruoff, "Tunable electrical conductivity of individual graphene oxide sheets reduced at low temperatures," Nano Lett. **8**, 4283–4287 (2008).
[14]K. P. Loh, Q. Bao, G. Eda, and M. Chhowalla, "Graphene oxide as a chemically tunable platform for optical applications," Nat. Chem. **2**, 1015–1024 (2010).
[15]S. Stankovich, D. A. Dikin, G. H. B. Dommett, K. M. Kohlhaas, E. J. Zimney, E. A. Stach, R. D. Piner, S. T. Nguyen, and R. S. Ruoff, "Graphene-based composite materials," Nature **442**, 282–286 (2006).
[16]H. A. Becerril, J. Mao, Z. Liu, R. M. Stoltenberg, Z. Bao, and Y. Chen, "Evaluation of solution-processed reduced graphene oxide films as transparent conductors," ACS Nano **2**, 463–470 (2008).
[17]Y. Zhu, S. Murali, M. D. Stoller, K. J. Ganesh, W. Cai, P. J. Ferreira, and A. Pirkle, "Carbon-based super-capacitors produced by activation of graphene," Science **332**, 1537–1541 (2011).
[18]Y. Zhu, S. Murali, M. D. Stoller, A. Velamakanni, R. D. Piner, and R. S. Ruoff, "Microwave assisted exfoliation and reduction of graphite oxide for ultracapacitors," Carbon **48**, 2118–2122 (2010).
[19]G. Eda, G. Fanchini, and M. Chhowalla, "Large-area ultrathin films of reduced graphene oxide as a transparent and flexible electronic material," Nat. Nanotechnol. **3**, 270–274 (2008).
[20]R. Maiti, S. Manna, A. Midya, and S. K. Ray, "Broadband photoresponse and rectification of novel graphene oxide/n-Si heterojunctions," Opt. Express **21**, 26034–26043 (2013).
[21]D. Yang, A. Velamakanni, G. Bozoklu, S. Park, M. Stoller, R. D. Piner, and S. Stankovich, "Chemical analysis of graphene oxide films after heat and chemical treatments by X-ray photoelectron and micro-Raman spectroscopy," Carbon **47**, 145–152 (2009).
[22]K. A. Mkhoyan, A. W. Contryman, J. Silcox, D. A. Stewart, G. Eda, C. Mattevi, S. Miller, and M. Chhowalla, "Atomic and electronic structure of graphene-oxide," Nano Lett. **9**, 1058–1063 (2009).
[23]G. Eda, Y. Lin, C. Mattevi, H. Yamaguchi, H. Chen, I. Chen, C. Chen, and M. Chhowalla, "Blue photoluminescence from chemically derived graphene oxide," Adv. Mater **22**, 505 (2010).
[24]S. Pei and H. M. Cheng, "The reduction of graphene oxide," Carbon **50**, 3210–3228 (2012).
[25]Z. Liu, Y. Wang, X. Zhang, Y. Xu, Y. Chen, and J. Tian, "Nonlinear optical properties of graphene oxide in nanosecond and picosecond regimes," Appl. Phys. Lett. **94**, 021902 (2009).
[26]X. Jiang, L. Polavarapu, S. T. Neo, T. Venkatesan, and Q. Xu, "Graphene oxides as tunable broadband nonlinear optical materials for femtosecond laser pulses," J. Phys. Chem. Lett. **3**, 785–790 (2012).
[27]X. Zhao, Z. Liu, W. Yan, Y. Wu, X. Zhang, Y. Chen, and J. Tian, "Ultrafast carrier dynamics and saturable absorption of solution-processable few-layered graphene oxide," Appl. Phys. Lett. **98**, 121905 (2011).
[28]C. V. Pham, S. Repp, R. Thomann, M. Krueger, S. Weber, and E. Erdem, "Charge transfer and surface defect healing within ZnO nanoparticle decorated graphene hybrid materials," Nanoscale **8**, 9682 (2016).
[29]H. Shi, C. Wang, Z. Sun, Y. Zhou, K. Jin, S. A. T. Redfern, and G. Yang, "Tuning the nonlinear optical absorption of reduced graphene oxide by chemical reduction," Opt. Express **22**, 19375–19385 (2014).
[30]J. Hummers, S. William, and R. E. Offeman, "Preparation of graphitic oxide," J. Am. Chem. Soc. **80**, 1339–1339 (1958).
[31]R. Maiti, A. Midya, C. Narayana, and S. K. Ray, "Tunable optical properties of graphene oxide by tailoring the oxygen functionalities using infrared irradiation," Nanotechnology **25**, 495704 (2014).
[32]H. Guo, M. Peng, Z. Zhu, and L. Sun, "Preparation of reduced graphene oxide by infrared irradiation induced photothermal reduction," Nanoscale **5**, 9040 (2013).
[33]F. Kim, J. Y. Luo, R. Cruz-Silva, L. J. Cote, K. Sohn, and J. X. Huang, "Self-propagating domino-like reactions in oxidized graphite," Adv. Funct. Mater. **20**, 2867–2873 (2010).
[34]J. T. Robinson, S. M. Tabakman, Y. Liang, H. Wang, H. S. Casalongue, D. Vinh, and H. Dai, "Ultra small reduced graphene oxide with high near-infrared absorbance for photothermal therapy," J. Am. Chem. Soc. **133**, 6825–6831 (2011).
[35]M. Sheik-Bahae, A. A. Said, T. H. Wei, D. J. Hagan, and E. W. Van Stryland, "Sensitive measurement of optical nonlinearities using a single beam," IEEE J. Quantum Electron. **26**, 760–769 (1990).
[36]A. Bateni, E. Erdem, S. Repp, S. Acar, I. Kokal, W. Häßler, S. Weber, and M. Somer, "Electron paramagnetic resonance and Raman spectroscopy studies on carbon-doped MgB2 superconductor nanomaterials," J. Appl. Phys. **117**, 153905 (2015).
[37]C. V. Pham, M. Krueger, M. Eck, S. Weber, and E. Erdem, "Comparative electron paramagnetic resonance investigation of reduced graphene oxide and carbon nanotubes with different chemical functionalities for quantum dot attachment," Appl. Phys. Lett. **104**, 132102 (2014).
[38]S. Yumitori, "Correlation of C1s chemical state intensities with the O1s intensity in the XPS analysis of anodically oxidized glass-like carbon samples," J. Mater. Sci. **35**, 139–146 (2000).
[39]I. Childres, L. A. Jauregui, and Y. P. Chen, "Raman spectra and electron-phonon coupling in disordered graphene with gate-tunable doping," J. Appl. Phys. **116**, 233101 (2014).
[40]H. Kang, A. Kulkarni, S. Stankovich, R. S. Ruoff, and S. Baik, "Restoring electrical conductivity of dielectrophoretically assembled graphite oxide sheets by thermal and chemical reduction techniques," Carbon **47**, 1520–1525 (2009).
[41]J. I. Paredes, S. Villar-Rodil, A. Martinez-Alonso, and J. M. D. Tascon, "Graphene oxide dispersions in organic solvents," Langmuir **24**, 10560–10564 (2008).
[42]D. Li, M. B. Mueller, S. Gilje, R. B. Kaner, and G. G. Wallace, "Processable aqueous dispersions of graphene nanosheets," Nat. Nanotechnol. **3**, 101–105 (2008).
[43]L. Huang, Y. Liu, L. Ji, Y. Xie, T. Wang, and W. Shi, "Pulsed laser assisted reduction of graphene oxide," Carbon **49**, 2431–2436 (2011).
[44]R. L. Sutherland, *Handbook of Nonlinear Optics* (Marcel Dekker, 1996).
[45]X. Zhang, Z. Liu, X. Li, Q. Ma, X. Chen, J. Tian, Y. Xu, and Y. Chen, "Transient thermal effect, nonlinear refraction and nonlinear absorption properties of graphene oxide sheets in dispersion," Opt. Express **21**, 7511–7520 (2013).
[46]J. Shang, L. Ma, J. Li, W. Ai, T. Yu, and G. G. Gurzadyan, "The origin of fluorescence from graphene oxide," Sci. Rep. **2**, 792 (2012).
[47]L. Liu, L. Wang, J. Gao, J. Zhao, X. Gao, and Z. Chen, "Amorphous structural models for graphene oxides," Carbon **50**, 1690–1698 (2012).
[48]J. Robertson and E. P. O'reilly, "Electronic and atomic structure of amorphous carbon," Phys. Rev. B **35**, 2946 (1987).
[49]C. Mathioudakis, G. Kopidakis, P. C. Kelires, P. Patsalas, M. Gioti, and S. Logothetidis, "Electronic and optical properties of a-C from tight-binding molecular dynamics simulations," Thin Solid Films **482**, 151–155 (2005).
[50]P. K. Datta, S. Mukhopadhyay, G. K. Samanta, S. K. Das, and A. Agnesi, "Realization of inverse saturable absorption by intracavity third-harmonic generation for efficient nonlinear mirror mode-locking," Appl. Phys. Lett. **86**, 151105 (2005).